An Analysis of Pump Cavitation Damage

Michael C. Brophy,* David R. Stinebring† and Michael L. Billet‡
The Pennsylvania State University, State College, Pennsylvania

A method to predict the extent of cavitation damage occurring in the Space Shuttle Main Engine high-pressure oxidizer turbopump (HPOTP) was developed. A computational analysis was performed to solve for the complicated flow through the high-speed turbopump. The viscous effects of the blade boundary layers were included in the analysis. A three-dimensional map of the flowfield at the inducer inlet was obtained and a prediction of the resulting cavitation patterns on the inducer was made. The calculations show that unsteady blade surface cavitation is produced by the large incidence changes at the leading edge of the inducer, caused by the wakes of the upstream stationary vanes. Very high cavitation damage rates are associated with this type of cavitation. Recommendations are made that may significantly reduce this type of cavitation, and thus increase the operating life of the HPOTP.

Nomenclature

ℓ/c = vane length-to-chord ratio
P_∞ = local reference pressure
P_v = bulk liquid vapor pressure
r = radial coordinate
R/R_{tip} = nondimensional radius
V = velocity
V_∞ = reference velocity
W_c = velocity along the cavity wall
W_∞ = local relative velocity within inducer blade row
x = flow direction coordinate in the transformed plane
y = normal coordinate in the transformed plane
$\Delta\theta$ = angular or circumferential increment
$\Delta\psi$ = increment of stream function
θ = circumferential coordinate
π = circular constant
ρ = mass density of the working fluid
σ = cavitation number
ψ = stream function

Subscripts

r = radial direction
x = flow direction in the transformed plane
y = normal direction in the transformed plane
θ = circumferential direction

Introduction

THE destructive action caused by cavitation has long been a problem of practical importance with fluid machinery. The study of cavitation damage involves both solid mechanics and fluid mechanics of two-phase flows, and thus is inherently difficult. The problems associated with the occurrence of severe cavitation damage in fluid handling machinery are dependent primarily on the degree and type of cavitation. Pumps can operate with a limited degree of cavitation and still provide satisfactory performance although damage can possibly occur if operated over long periods of time.

The practical problem addressed herein is the reduction of the severe cavitation damage in the Space Shuttle Main Engine (SSME) high-pressure oxidizer turbopump (HPOTP) and the subsequent improvement of its life expectancy. Although the Space Shuttle program has been extremely successful, it has been so only at the cost of increased maintenance of these turbopumps. In the area of performance these engines have done exceedingly well, but they have yet to meet the overall mission requirement of long life. Extensive cavitation damage has been reported in only 30 min of operation, falling short of the desired life expectancy of 7.5 h. The Space Shuttle program is the first to require repeated usage of major engine components.

At the 109% power level the HPOTP operates at a speed of 30,000 rpm and produces nearly 21,000 kW of power. At full power level over 230 liters/s of liquid oxygen flow through each side of the double-suction pump. A headrise of over 2700 m is produced by increasing the pressure from approximately 2700 kPa to over 33,000 kPa. A cross-sectional view of the HPOTP is shown in Fig. 1 with its five blade row components identified. The flow enters from the pipe at the top of the figure and, after being split in two, passes through large stationary vanes (1) in the inlet casing and smaller stator vanes (2). It then turns a sharp 90-deg corner before entering the inducer (3). The inducer operates with appreciable amounts of cavitation, but provides sufficient headrise to prevent blade surface cavitation in the pump impeller (4). The flow is then collected in a volute after turning 90 deg in the impeller and passing through a set of stationary diffuser vanes (5). The volute exits to the pipe at the bottom of the figure. Also shown in Fig. 1 is a cross section of the turbine (to the right) which provides power to run the pump and also a boost pump (to the left).

In order to address the cavitation damage problem it was first necessary to obtain a prediction of the flowfield within the pump. A prediction of the cavitation extent can then be made from the velocity and pressure data obtained from the flow analysis. The development of a computational method to predict the three-dimensional flowfield at the inducer inlet and the resulting cavitation analysis is summarized herein. A more detailed presentation of the analysis is contained in Ref. 1.

An examination of the turbopump hardware has shown that the most severe cavitation damage occurs on the housing, downstream of the stator vanes and near the leading edge of the inducer. The damage appears as discrete spots at this loca-

Received Dec. 3, 1984; revision received July 22, 1985.

*Research Assistant, Applied Research Laboratory.
†Research Assistant, Applied Research Laboratory. Member AIAA.
‡Senior Research Associate, Applied Research Laboratory. Member AIAA.

tion and as a band of less severe damage toward the trailing edge of the inducer (see Fig. 2). The deep-pitting cavitation damage occurring on the housing significantly reduces the life expectancy of the turbopump.

High damage rates can be expected in this area because of the high inducer tip speed that is nearly 200 m/s. Many investigators, such as Knapp[2] and Stinebring,[3] have shown that the damage is proportional to the sixth power of the fluid velocity relative to the blade. The existence of deep pitting suggests that bubble collapse is occurring predominantly in this area. A circumferential variation in the amount of cavitation occurring on the inducer, resulting from a changing flow incidence angle, is shown to be the cause of this problem.

Inviscid Flow Analysis

The flow through the HPOTP is very complicated and the design of its components is critical. It consists of five blade rows, three of which are stationary, and the flow is turned four times in a very short distance. The flow analysis begins with an examination of the first two blade rows.

The inlet casing is a very difficult component to analyze. Flow enters through a pipe and is split in half to form a double-suction entrance (Fig. 1). The flow is then divided again in each side inlet (left and right), and is thus symmetric about a vertical axis, but each side inlet is asymmetric about the axis of rotation, as illustrated in Fig. 3.

Since flow through the inlet casing is predominantly radial for the stationary vane rows, a two-dimensional (2-D) approximation for the inlet casing boundary (vane 1), the inlet casing vanes (2-14), and the stator vanes (15-18) was chosen. The fifth stator vane at the bottom of the inlet (between vanes 16 and 17) has been blended into the casing boundary and provides for vertical symmetry of the flow in the inlet. It is still impractical, however, to solve for the flow in the configuration. A transformation must be performed to convert this radial flow geometry into a linear cascade geometry.

It is possible, however, to solve for the flow in the casing alone if all of the stationary vanes (2-18) are removed. The resulting singly connected domain can be solved by using a finite element method. The finite element solution is illustrated in Fig. 4. The streamlines that are plotted represent equal increments of flow. It can be seen that the flow is uniform at the inlet and exit, but at the indicated radii a substantial circumferential component of the flow is shown to exist. It will be the task of the stationary vanes to remove this circumferential velocity.

The solution technique employed to solve for the 2-D configuration with vanes is the Modified Douglas Neumann Cascade Program.[4] The original Douglas Neumann Cascade Program was developed by the Douglas Aircraft Corporation[5]

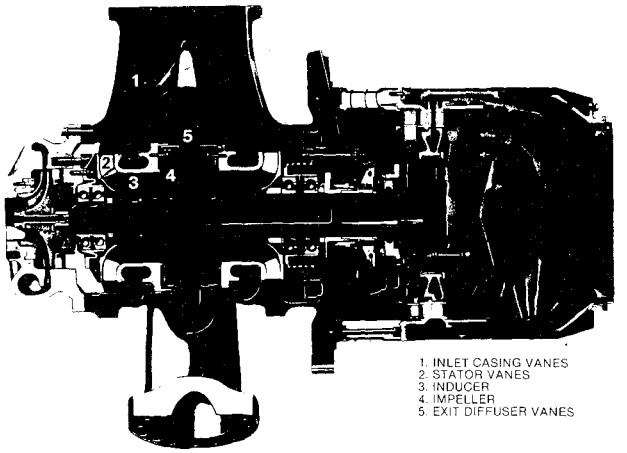

Fig. 1 Cross-sectional view of the high-pressure oxidizer turbopump (Rocketdyne).

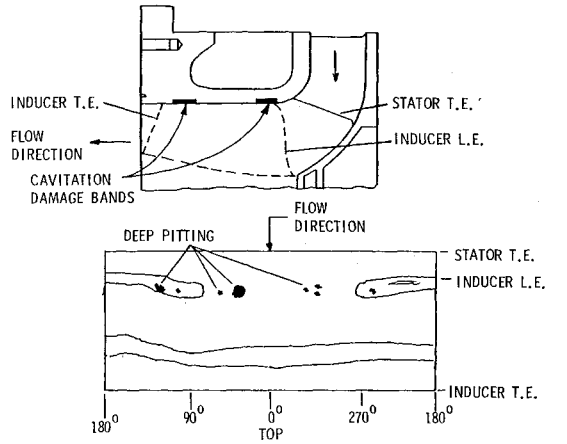

Fig. 2 High-pressure oxidizer turbopump cavitation damage on the housing (Rocketdyne).

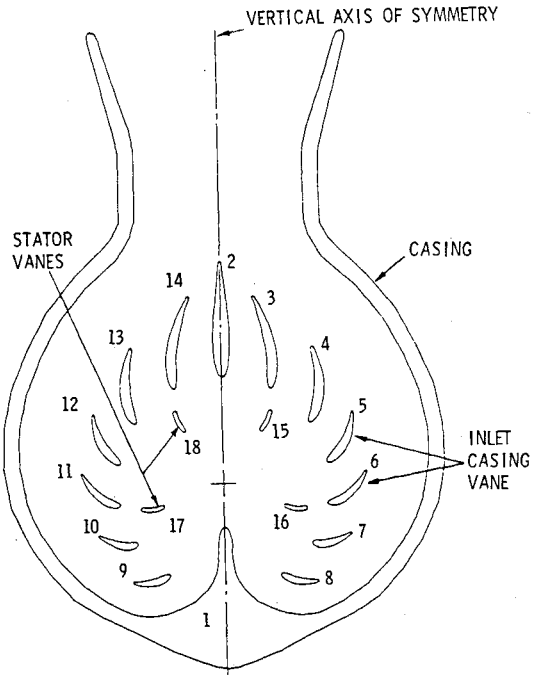

Fig. 3 Two-dimensional model of one side of the inlet casing.

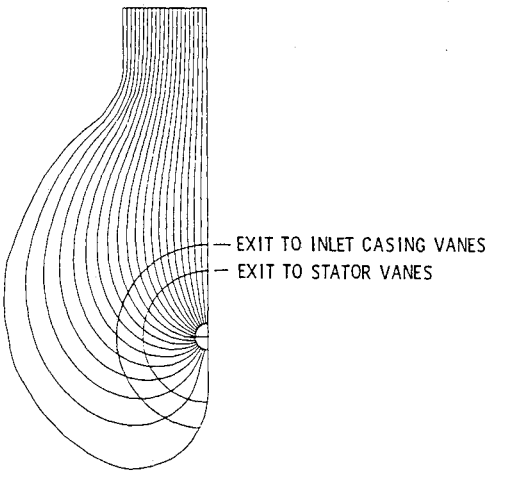

Fig. 4 Finite element flow solution for the inlet casing alone.

and extended the existing solution technique used for isolated airfoils to cascades of lifting or nonlifting bodies. The program has been modified further to include cascades with radial flow, either inward or outward, and radial flow cascades (r,θ) with bodies of varying geometry. Radial flow cascades are solved by transforming them into linear cascades (x,y) using a conformal transformation:

$$x=\ell n(r), \qquad y=\theta \tag{1}$$

Velocities calculated for the linear cascade are converted to the radial flow plane by simply dividing by the radius

$$V_r=\frac{1}{r}(V_x), \qquad V_\theta=\frac{1}{r}(V_y) \tag{2}$$

Special considerations must be employed to account for the inlet casing boundary since one would not normally consider this element to be a body in a cascade.

If the inlet casing boundary shown in Fig. 3 were transformed using Eq. (1), the large body with the dotted lines shown in Fig. 5 would be produced. With the flow proceeding from left to right, it can be seen that a large portion of the flow (approximately eleven-twelfths) would be blocked by the inlet casing, body 1. This is due to the flow entering the casing through the vertical inlet which accounts only for about 30 deg of the circumference. Therefore, it is adequate to represent the inlet casing boundary as the streamlined body shown in Fig. 5 to facilitate the flow calculation procedure. With this modification, the flow through the vertical inlet of Fig. 3 will still match the flow in the inlet region between the cascade boundary and body 1 in Fig. 5.

The Modified Douglas Neumann Cascade Program was first run for only one body—the inlet casing boundary. The resulting flow solution was found to match the finite element solution exactly. The 13 inlet casing vanes and 4 stator vanes were then added to solve for the flow in the 2-D configuration of Fig. 3. Although the vanes are symmetric about a vertical axis, each vane is unique when plotted in the tranformed plane. The entire geometry illustrated in Fig. 5 would be repeated at the top and bottom to form an infinite linear cascade. The inlet flow angle was set equal to zero to reflect this symmetry.

The flow solution for the existing inlet when transformed into the radial plane is illustrated in Fig. 6. When compared with the solution for the inlet casing boundary alone it was seen that the vanes had indeed taken out a large portion of the turning. However, a substantial amount of circumferential velocity still exists, which will have a marked effect on the inlet flow at the inducer.

The flow through the entire cross section of the HPOTP can be analyzed using a streamline curvature method (SCM).[6] The SCM program solves the continuity, momentum, and energy equations for the real variables: velocities and pressure. In the process, the streamline locations are found as well. The streamline curvature solution is illustrated in Fig. 7. The locations of the blade rows are highlighted, including the split impeller blades in the rotor. The exit diffuser vanes were omitted for this analysis, but could have easily been included. The flow solution illustrated in Fig. 7 is for the through-flow analysis only and must be combined with the Douglas Neumann circumferential solution to obtain the 3-D picture of what is happening at the inducer inlet.

It now becomes necessary to describe the flow along the various streamlines in Fig. 7 as the flow turns the corner. There are three locations of primary importance in this part of the analysis: 1) the exit of the inlet casing vanes, 2) the exit of the stator vanes, and 3) the probe location within the inducer area, where experimental data were previously obtained. The corresponding stations for the SCM solution are shown in Fig. 7 as numbers 12, 18, and 22. The flow is computed at these locations as it turns the corner.

The first location illustrates the flow as it exits the inlet casing vane row and enters the stator vane row. Here the flow is assumed radial and is calculated from the Douglas Neumann solution of the vane geometry in Fig. 3. In a similar manner, the second location illustrates the flow exiting the stator vane row. For both of these locations the radial velocity is integrated to check on the mass flow. When the integration is performed, the stream function is calculated as a function of circumferential location:

$$\Delta\psi=r\sum_{0}^{\pi}V_r\Delta\theta \tag{3}$$

These values are normalized by the design mass flow to produce values of the stream function from zero to one as θ increases from 0 to π rad. Since constant values of ψ represent streamlines, the location of a selected fluid particle can be calculated at each of the two radii. This links up the locations of importance on each stream surface as the flow turns the corner.

The third location within the inducer area, where experimental data are available, is analyzed in a similar fashion with two major exceptions. First, the streamline changes from the radial to the axial direction, which results in a different average through-flow velocity with which to normalize the

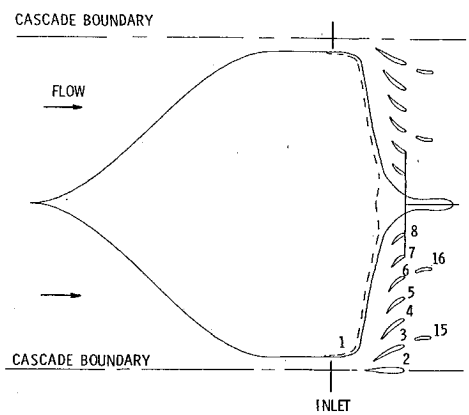

Fig. 5 Transformed cavity with guide vanes.

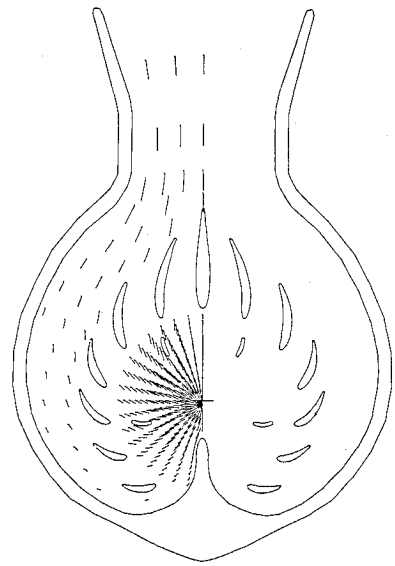

Fig. 6 Flow solution for the casing with guide vanes.

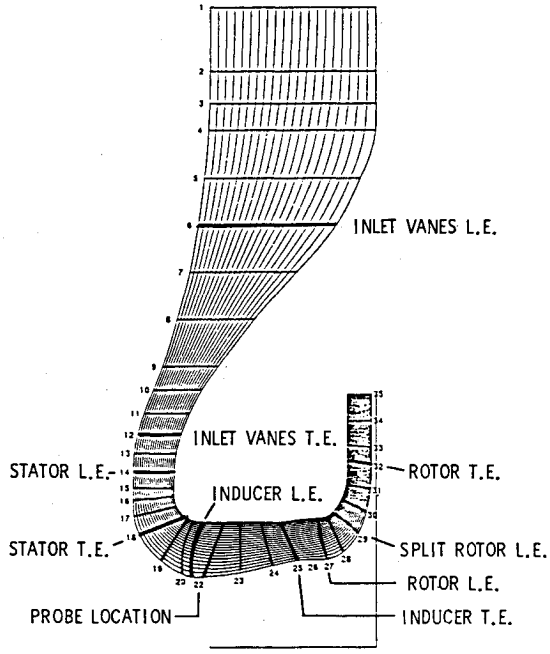

Fig. 7 Streamline curvature solution for the flow through the turbopump.

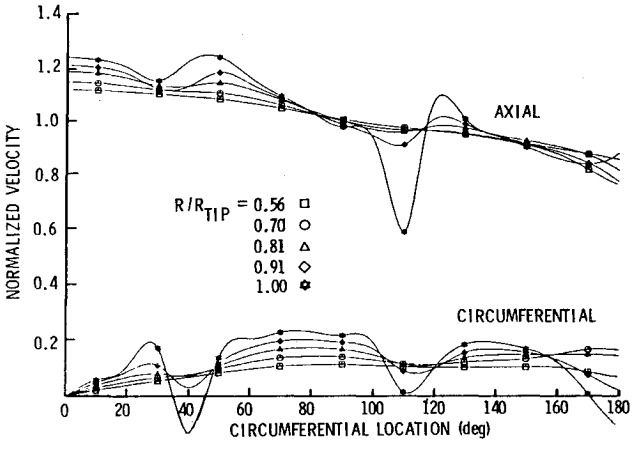

Fig. 8 Inviscid flow solution at the inducer (station 22).

flow due to area changes. Second, the law of constant angular momentum, which is employed in the SCM, cannot be used for this portion of the analysis. As the fluid particles change radius from that at the stator vane exit to that of the inducer inlet, the casing will continue to act on them and produce a variation in the angular momentum of the fluid around the circumference.

The potential flowfield at the inducer (station 22) is depicted in Fig. 8. There is a noticeable indication of blockage at the two stator locations at radii toward the tip streamline. This results from the close proximity of the stator vanes and the inducer leading edge at the outer tip boundary. It is also important to note that the mass flow falls off toward the bottom of the inlet, which would be expected for flow entering at the top.

Addition of the Viscous Effects to the Inviscid Flow Analysis

The viscous boundary-layer growth on the stationary blade rows will lead to fluid deviation and wake velocity deficits

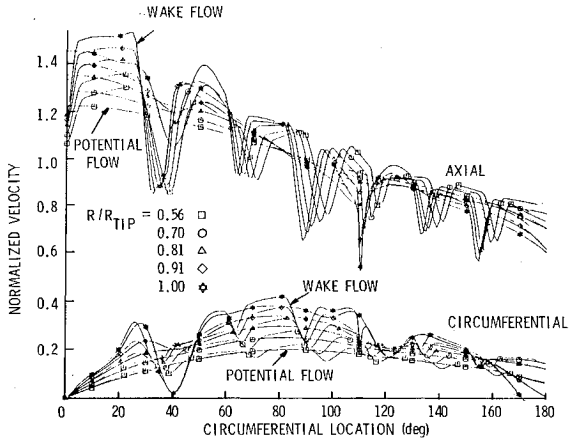

Fig. 9 Complete flow solution at the inducer (station 22).

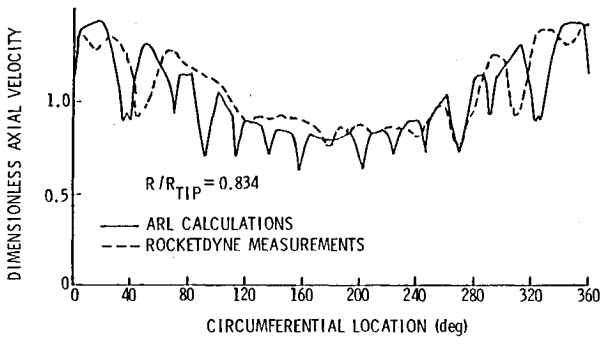

Fig. 10 Comparison of measured and calculated axial velocity profiles at the inducer inlet.

downstream of the vanes. These effects can readily be included in the flow analysis. In real fluid flow, turning vanes will always achieve less turning than that indicated by their camber lines. The fluid will not exit at the blade angle, but at a lesser angle. In the inviscid analysis the flow is constrained by the Kutta condition to exit at the specific trailing-edge angle. In order to achieve the proper flow condition downstream of the vane rows, the fluid deviation must be added to the inviscid calculation. This was accomplished by fixing the vanes at the leading edge and increasing the stagger angle to force the flow to exit at the deviated flow angle.

The deviation angle was estimated from the blade incidence angle obtained from the inviscid flow analysis, taking into account camber, blade thickness, and flow acceleration. The deviations due to camber and blade thickness were obtained by utilizing empirical data collected by Lieblein.[7] The work by Lakshminarayana[8] was used to estimate the deviation due to flow acceleration. It is important to note that cascade relationships were used to estimate the deviation angles for the vanes inside the casing. However, since all of the vanes in the HPOTP are of different geometry, the calculated deviation angles are only approximate. As expected, the resulting Douglas Neumann solution indicated an even greater disparity of the mass flow from top to bottom of the inlet when deviation angles were included in the analysis. Also due to viscous effects, the casing vanes failed to reduce the tangential velocity as much as before.

The calculated wakes were also added to the flow at the exit of each of the stationary vanes. Effectively, the potential velocity distribution is multiplied by a wake deficit factor that will be greater than 1 between vanes and less than 1 in the proximity of the vane trailing edge. The wakes will have different widths and depths due to the process of accounting for the wake diffusion prior to reaching the inducer leading edge.

From Fig. 7, it should be obvious that the wakes at the hub streamline will be able to diffuse (or decay) prior to entering the inducer, whereas the wakes at the tip streamline will remain narrow and deep. The wakes were diffused by introducing the steamwise distance between the vane exit station and the inducer station.

The far-wake equations were used to calculate the velocity profile using the mixing-length concept of Schlichting.[9] The drag coefficient based on the momentum thickness needed in this calculation was obtained by applying Truckenbrodt's energy integral method[10] for the turbulent boundary layer with a pressure gradient. After the wake profiles were calculated, they were repositioned at the trailing edge of the casing vanes. The mass flow at this location is then corrected for the wake blockage by integrating over the circumference.

By making use of the stream function in the circumferential direction, the flow is again calculated downstream. Thus the wakes from the inlet casing vanes are transferred to the stator vane exit location and, because of the residual tangential velocity, are shifted to larger values of θ. In several cases the two wakes combine to complicate the flow. For each of the wake flow distributions the mass flow is integrated and checked. The curves at different radii will not all reach 180 deg due to blockage by the boundary (fifth stator vane between 16 and 17 in Fig. 3) at that point. In a similar manner, the wakes are transferred to the inducer (station 22) in Fig. 9.

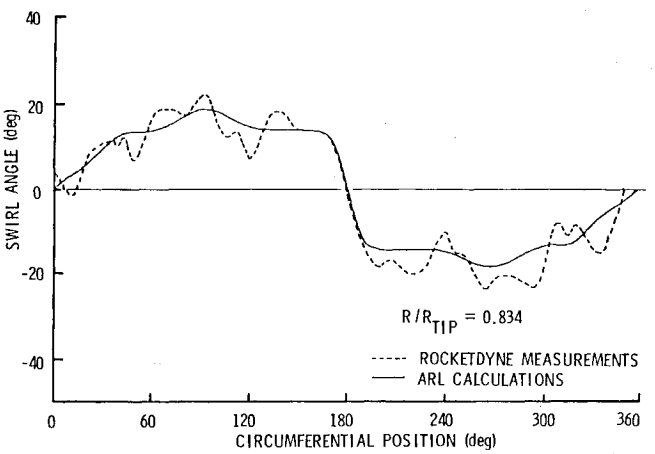

Fig. 11 Comparison of measured and calculated swirl angles at the inducer inlet.

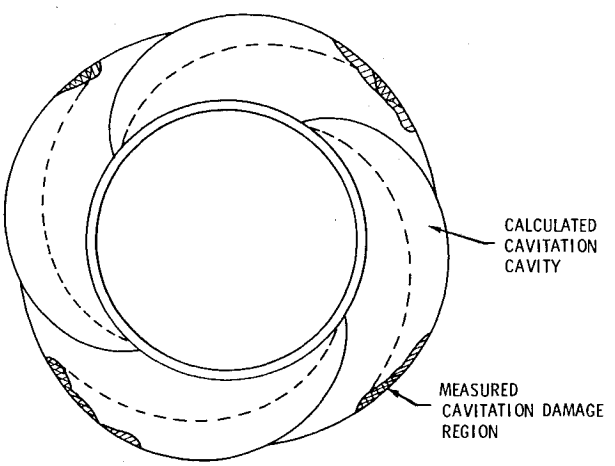

Fig. 12 Location of cavitation damage on the inducer together with the calculated cavitation pattern for uniform flow and no preswirl.

Experimental Verification of the Analysis

The prediction of the inlet flow to the inducer is a critical part of the damage analysis. The computational procedure has several key assumptions that need to be verified. The flow solution given in Fig. 9 shows that the inducer inlet flow is nonuniform, producing large incidence variations that result in unsteady cavitation. This type of cavitation causes severe cavitation damage and high unsteady forces.

Rocketdyne conducted a series of experiments on the SSME HPOTP inlet in air.[11] For these experiments, a 5-hole probe[12] was utilized to obtain flow data in the inducer at station 22. Total and static pressure, axial velocity, and swirl angle were obtained as a function of circumferential angle.

A comparison is given in Fig. 10 for the axial velocity and in Fig. 11 for the swirl angle at a nominal radius. For this comparison the Rocketdyne data were integrated to obtain an average velocity which then was used to normalize the data. These results are in excellent agreement.

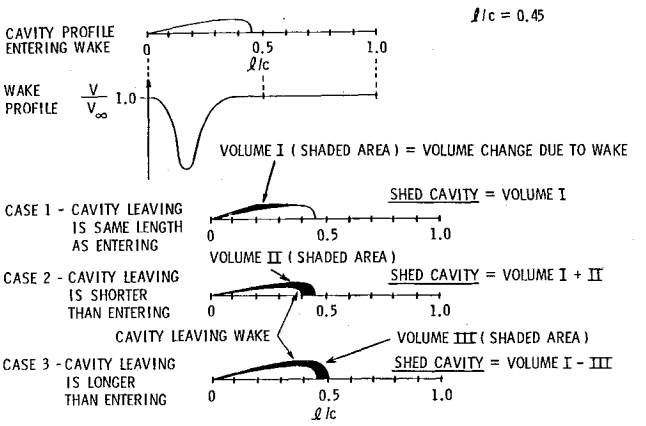

Fig. 13 Method for the calculation of a shed cavity through a wake.

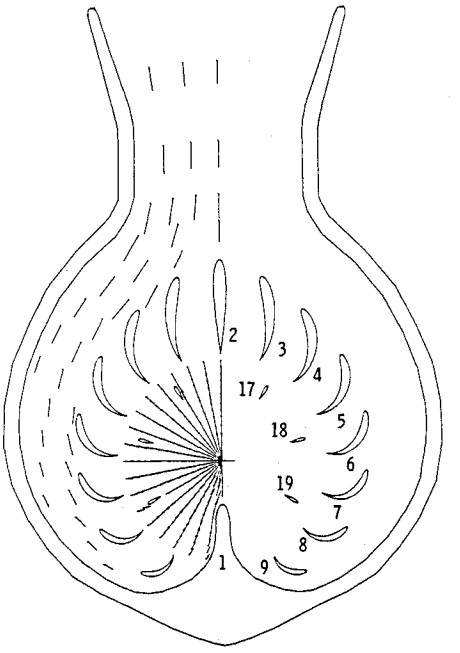

Fig. 14 Potential flow solution for the altered vanes.

Cavitation Analysis of the Existing Design

The damage that currently limits the life of the pump is the deep pitting on the inducer casing which is concentrated downstream of the stator vanes. The damage could not be due to cavitation on the stator vanes, since the local cavitation number is too high for cavitation to occur. For the flow over the stator vanes the cavitation number can be defined as

$$\sigma = \frac{P_\infty - P_v}{\frac{1}{2}\rho V_\infty^2} \tag{4}$$

where P_∞ and V_∞ are the local values of static pressure and velocity, ρ the mass density of the working fluid, and P_v the bulk liquid vapor pressure. At the trailing edge of the stator vanes σ was calculated to be 4.7. This is much too high for any significant amount of cavitation. The damage must be due to other causes.

The local cavitation number on the inducer blade can be defined as

$$\sigma = \frac{P_\infty - P_v}{\frac{1}{2}\rho W_\infty^2} \tag{5}$$

where W_∞ is the local relative velocity of the blade section. For uniform flow and no preswirl at the inducer, $\sigma = 0.108$ was calculated at the blade tip. With a blade angle of 13.12 deg ($r = 2.32$ in.), the relative flow angle is 4.3 deg and the cavity length is approximately 33% of the chord length, as calculated by the method of Stripling and Acosta.[13] At the hub, $\sigma = 0.318$ and the cavity length was calculated to be only 7% of the chord length. The calculated cavitation pattern for this "steady-state" condition is superimposed upon the measured damage on the inducer blades and is presented in Fig. 12. As seen in the figure, the trailing edge of the cavity at the tip corresponds to the region of light damage on the blade. Also, the trailing edge of this calculated "steady-state" cavity is at the same axial location as the light band of damage about the circumference of the casing, shown in Fig. 2. But how then could the most severe damage be concentrated at certain areas on the casing?

To answer this question, the area in which the deep pitting damage is located provides part of the answer. In general, the deep pits are downstream of the stator vanes. It is probable that, given the close proximity to the inducer leading edge, the viscous wakes shed from the stator vanes could be disturbing the flow. A decrease in axial velocity would increase the relative flow angle and, thus, the amount of cavitation. As the inducer blades pass through these wakes, some of the cavity is shed and the resulting cavity collapses are creating the damage.

There are a number of reasons why it is thought that part of the cavity breaks off due to the wake rather than just causing a fluctuation in cavity length. First, the velocity at the inducer blade tip is nearly 200 m/s and the time to traverse a 20-deg wide wake is approximately 0.1 ms. The cavity would not have time to reach a "steady-state" condition. Second, if the wake causes only a cavity length fluctuation there should be severe damage to the inducer blade. This was not the case. Finally, observations of some propeller blades with sharp leading edges operating in a wake flow show a similar cavity behavior.[15]

A method was developed to estimate the volume shed from the cavity as an inducer blade passes through each wake from the upstream vanes. It will be assumed that:

1) A steady-state cavity is reached before the blade enters a wake and that a steady-state cavity will exist some time after the blade passes through the wake.

2) A disturbance generated along the cavity wall will propagate with a velocity of $W_c = W_\infty\sqrt{1+\sigma}$, which is the velocity along the free surface bounding the cavity.

3) The disturbance in the cavity will follow a path corresponding to the flow at the leading edge where the disturbance was produced.

4) The cavitation number is nearly constant through the wake.

As a blade with a steady-state cavity starts to move through a wake, the blade will see a fluctuating flow angle due to the reduced axial and tangential velocity at each position. Therefore, the change in incident flow angle will create a disturbance at the leading edge of the cavity. The disturbance will propagate at the fluid velocity along the cavity wall. The magnitude and direction of the velocity vector at the leading edge are functions of the position in the wake. If the width of the wake is less than the length of the cavity on the blade as it enters the wake, then the blade leading edge will reach the other sides of the wake before the initial disturbance to the cavity shape reaches the cavity trailing edge. This is important since for the wake cavity model there is no closure condition specified at the trailing edge. A closure condition could be specified but it is not required for the cases that will be investigated on the inducer blade.

The "perturbed" cavity shape and shed volume can be calculated by the following procedure:

1) The inducer blade leading edge is placed at the exit point of the wake.

2) The flow angle and velocity at any point through the wake are used to calculate the cavity contour at the same point on the blade.

3) The volume of the shed cavity is equal to the difference between the volume of the perturbed and steady-state cavities.

Qualitatively, the results of such an analysis are shown in Fig. 13.

The shed cavity comes from two sources: the perturbation to the original cavity due to the wake, and the fact that the cavity volume will likely change even from the incident steady-state condition from one side of the wake to the other. A decrease in the cavity length occurs upon leaving the wake on the counterswirl side since the axial velocity is increasing as the inducer blades move from 180 to 0 deg. When the inducer blades move from 0 to 180 deg the opposite is true. The cavity leaving the wake is typically larger than the cavity on the blade when entering the wake. Some of the volume in the "perturbed" cavity must be used to "fill" the cavity leaving the wake. If the wake is not very "severe," there may be no shed cavity at all.

For both preswirl and counterswirl sides, the heaviest pitting was downstream of inlet casing vane 3 and stator vane 15 (Fig. 3). The steady-state cavities entering and leaving the wake are small (less than 0.1 ℓ/c) for both preswirl and counterswirl sides. Thus nearly all of the cavity volume generated while the blade was in the wake would be shed, resulting in the severe damage rates experienced by the HPOTP.

Emphasis has been on damage from unsteady cavitation created when the inducer enters a wake. As indicated in the literature,[14,15] this type of damage is at least an order of magnitude greater than its steady cavitation counterpart.

Recommendations for Cavitation Damage Reduction

The analysis of the existing stationary vanes in the HPOTP clearly indicates that the vanes must be altered to improve the turbopump's cavitation performance and, hence, reduce cavitation damage. Several theoretical modifications were made to the existing vane geometry and a comparison of the predicted cavitation damage rates was obtained. These modifications strive to minimize the fluid turning at the inducer, equalize the mass flow around the circumference of the inlet, and reduce the sensitivity to flow incidence by altering the vane shapes.

Due to the uncertainty in the exact angle at which the flow will encounter the vane at the leading edge, a rounded surface

should be used to allow the flow to pass beyond the leading edge minimizing the possibility of flow separation on either the pressure or suction surface. The trailing edge should be made as thin as possible for the same reason. An NACA 65-0012 series vane shape was selected as a possible candidate for the modified vanes. The camber offset was increased for each vane until the desired amount of turning was produced.

The Douglas Neumann Cascade Program solves for the flow at any location in the cascade. Although the flow *at* the trailing edge must be tangent to the vanes, the inviscid flow *between* the vanes can still exhibit a substantial degree of turning different from that indicated by the adjacent vanes. Thus some overturning may be required to direct the flow radially at the exit of the stationary vanes on the average. New stationary vane shapes were configured in an attempt to reduce the wakes and, thus, the unsteady cavitation.

The stator vanes serve no useful purpose hydrodynamically. While they might be important structurally, their presence in the flowfield serves only to aggravate the situation at the inducer because of their close proximity. Six vanes were employed in the new analysis instead of four, but each is one-third shorter than the original vanes. The actual number and size of these vanes would be dictated by structural considerations. While the new stator vanes will divert the flow locally, they will have minimal impact on the flow at the inducer and could readily be removed from the analysis.

The inlet casing vanes were increased in number from 13 to 15. This would serve to maintain force levels on each vane since more turning will now be expected of the vane row to eliminate the tangential component of the velocity. They were spaced equally at their trailing edge between the tip and bottom of the casing boundary. The amount of turning used for each vane was computed to allow the flow to enter the vane row with no appreciable incidence and to exit radially. In some cases fluid turning angles close to 90 deg were indicated. This is typical for inlets of this type where the flow is first directed tangentially by the casing near the upper inlet and then must be turned radially.

The vane were decreased uniformly in chord length from the top casing vane, No. 2, to the bottom vane, No. 9. Vertical symmetry was employed to minimize the side forces on the shaft. Obviously the downward force will still be substantial. The inviscid flow was calculated to produce radial flow at the radii corresponding to the inducer station, thereby eliminating any circumferential velocity.

The flow solution and new vane shapes are illustrated in Fig. 14. The flowfield at the inducer (station 22) is shown in Fig. 15. With the reduction of the circumferential velocity the flow becomes more uniform at the inducer and the circumferential mass flow distribution is nearly constant. Note that the casing boundary is still responsible for some fluid turning toward the bottom of the inlet at large values of θ. This turning can be removed only by altering the bottom of the inlet casing.

As can be noted in Fig. 15, the deepest wakes are produced by the three stator vanes on each side. It appears that due to the location of these vanes (in close proximity to the inducer leading edge), the wakes will have the maximum velocity deficit and perphaps be the controlling factor for cavitation performance.

The cavity length calculations, based on the wakes with the maximum velocity deficit, for the new configuration with and without stator vanes were also performed. There were a number of improvements for both configurations over the existing turbopump. These can be summarized as follows:

1) The flow velocity is more uniform, thus the cavity lengths entering and leaving the wake are nearly equal.

2) The velocity deficit is reduced significantly for the redesign with no stator vanes.

3) The widths of the wakes are reduced.

The cavity volumes shed were calculated for an inducer blade traversing the wakes downstream of the modified casing

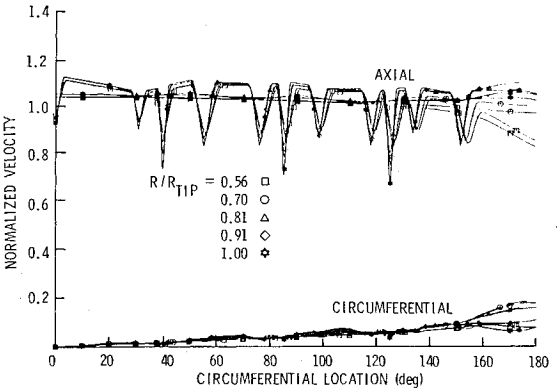

Fig. 15 Wake flow solution at the inducer (station 22) for the altered vanes.

blades. A comparison was then made with the existing design results. The comparison showed that for wakes with the greatest velocity deficit, for each configuration, the modified casing vanes of the Applied Research Laboratory of the Pennsylvania State University reduced the cavity volume shed by a factor of 21. If it is assumed that the rate of cavitation damage is proportional to the rate of shed cavity volume, then a pump with the modified inlet casing should be expected to have its operational lifetime extended by a factor of 21 over the present design.

In justifying the analogy between the damage and shed cavitites it must be mentioned that the only difference in the flow at the inducer, between the two configurations, is the difference in the magnitude of the wakes. The calculated mean velocity (mass flow), static pressure, and mean flow angle at the inducer (average about the circumference) were assumed unchanged. Also, it is assumed that both configurations are constructed of the same materials. The only difference between the two would be the volume of the cavities shed, collapsing at discrete locations about the circumference of the inducer housing.

Summary and Conclusions

A model has been developed that correlates the severe cavitation damage in the high-pressure oxidizer turbopump (HPOTP) with the inducer unsteady cavitation. A computational procedure was used to analyze the flow through the inlet casing including the prediction of wakes downstream of the casing vanes. The predicted flow at the inducer inlet compares very favorably with the experimental data obtained by Rocketdyne.

The analysis of the HPOTP clearly shows that the inlet casing vanes must be altered significantly to reduce the cavitation damage rate. However, any improvements should strive to reduce the vane sensitivity to flow incidence, equalize the distribution of the mass flow around the circumference of the inlet, minimize the swirl at the inducer inlet and, if possible, eliminate the stator vanes in front of the inducer.

Using the analytical method presented, a substantial reduction in the cavitation damage rate was predicted.

The following conclusions can be made:

1) The cavitation damage problem on the HPOTP results from the unsteady interaction of the inlet casing and stator vane wakes and the cavity flow over the inducer blades.

2) The existing vanes produce large wakes that combine to give severe velocity deficits at the leading edge of the inducer. Also, a significant amount of fluid turning exists downstream of the vanes.

3) The stator vanes should be removed, if possible, due to their close proximity to the inducer blades.

4) Changes to the inlet casing vanes are required to improve greatly the cavitation damage rate occurring on the housing.

5) The shape of the casing boundary should also be altered to act as a guiding surface at 180 deg from the vertical inlet.

An analysis was conducted which shows that the nonuniform flow entering the inducer causes the severe cavitation damage that exists in the HPOTP. Alterations to the stationary vanes were found to reduce significantly the cavitation damage rate. Recommendations were made that would improve the operating life of the HPOTP.

Acknowledgments

This work was sponsored under Contract NAS8-34535 from the George C. Marshall Space Flight Center. Mr. Glen Wilmer Jr. was the technical monitor of this program. The authors would like to thank Drs. R.E. Henderson and J.W. Holl on the staff of the Applied Research Laboratory for their very helpful discussions. Special appreciation is expressed to Dr. A.J. Acosta at the California Institute of Technology who served as a consultant.

References

[1]Brophy, M.C., Stinebring, D.R., and Billet, M.L., "A Study of Pump Cavitation Damage," NASA-CR-170992, Nov. 1983.

[2]Knapp, R.T., "Recent Investigations of Cavitation and Cavitation Damage," *Transactions of ASME,* Vol. 77, 1955, pp. 1045-1054.

[3]Stinebring, D.R., "Scaling of Cavitation Damage," M.S. Thesis, Applied Research Laboratory, The Pennsylvania State University, State College, PA, TM 76-51, Feb. 1976.

[4]Yocum, A.M., "A Computer Program for Calculating Potential Flow Solutions for Flow Through Linear and Stationary Circular Cascades," Applied Research Laboratory, The Pennsylvania State University, State College, PA, TM 81-130, June 1981.

[5]Giesing, J.P., "Extension of the Douglas Neumann Program to Problems of Lifting, Infinite Cascades," U.S. Department of Commerce, Washington, DC, Rept. LB31653, AD 605207, revised July 2, 1964.

[6]McBride, M.W., "A Streamline Curvature Method of Analyzing Axisymmetric Axial, Mixed and Radial Flow Turbomachinery," Applied Research Laboratory, The Pennsylvania State University, State College, PA, TM 77-219, July 1977.

[7]Lieblein, S.M., "Experimental Flow in Two-Dimensional Cascades," NASA SP-36, 1965.

[8]Lakshminarayana, B., Discussion of Wilson, Mani, and Acosta's "A Note on the Influence of Axial Velocity Ratios on Cascade Performance," NASA SP-304, Pt. I, 1974, pp. 127-133.

[9]Schlichting, J., *Boundary-Layer Theory*, 6th Ed., McGraw-Hill Book Co., New York, 1968, pp. 691-694.

[10]Truckenbrodt, E., *Boundary-Layer Theory,* 6th Ed., McGraw-Hill Book Co., New York, 1968, pp. 634-644.

[11]Cook, R.M., Private communication, Aerodynamics, Rocketdyne Division, Rockwell International, Canoga Park, CA, 83RC06062, June 9, 1983.

[12]Treaster, A.L. and Yocum, A.M., "The Calibration and Application of Five-Hole Probes," *ISA Transactions,* Vol. 18, No. 3, 1979, pp. 23-34.

[13]Stripling, L.B. and Acosta, A.J., "Cavitation in Turbopumps — Part I," *Transactions of ASME,* Vol. 84D, Sept. 1962, pp. 326-338.

[14]Cumming, R.A., Dashraw, F.J., and Hackworth, J.V., "An Investigation of the Effects of Wake Nonuniformity on Cavitation Erosion Damage of Propellers," *Proceedings of the Joint Symposium on Design and Operation of Fluid Machinery,* Colorado State University, Ft. Collins, CO, June 1978, pp. 497-509.

[15]Wilson, M.B., McCallum, D.N., Boswell, R.J., Bernhard, D.D., and Chase, A.B., "Cause and Corrections for Propeller-Excited Airborne Noise on a Naval Auxiliary Oiler," DTNSRDC 83/097, ADA135731, Nov. 1983.